Neurosci. **17,** 509–512 (1994).
5. Akaike, N., Krishtal, O. A. & Maruyama, T. Proton-induced sodium current in frog isolated dorsal root ganglion cells. *J. Neurophysiol.* **63,** 805–813 (1990).
6. Canessa, C. M., Horisberger, J. D. & Rossier, B. C. Epithelial sodium channel related to proteins involved in neurodegeneration. *Nature* **361,** 467–470 (1993).
7. Canessa, C. M. *et al.* Amiloride-sensitive epithelial Na^+ channel is made of three homologous subunits. *Nature* **367,** 463–467 (1994).
8. Lingueglia, E., Voilley, N., Waldmann, R., Lazdunski, M. & Barby, P. Expression cloning of an epithelial amiloride-sensitive Na^+ channel. A new channel type with homologies to *Caenorhabditis elegans* degenerins. *FEBS Lett.* **318,** 95–99 (1993).
9. Lingueglia, E. *et al.* Different homologous subunits of the amiloride-sensitive Na^+ channel are differently regulated by aldosterone. *J. Biol. Chem.* **269,** 13736–13739 (1994).
10. Lingueglia, E., Champigny, G., Lazdunski, M. & Barbry, P. Cloning of the amiloride-sensitive FMRFamide peptide-gated sodium channel. *Nature* **378,** 730–733 (1995).
11. Waldmann, R., Champigny, G., Bassilana, F., Voilley, N. & Lazdunski, M. Molecular cloning and functional expression of a novel amiloride-sensitive Na^+ channel. *J. Biol. Chem.* **270,** 27411–27414 (1995).
12. Driscoll, M. & Chalfie, M. The *mec-4* gene is a member of a family of *Caenorhabditis elegans* genes that can mutate to induce neuronal degeneration. *Nature* **349,** 588–593 (1991).
13. Huang, M. & Chalfie, M. Gene interactions affecting mechanosensory transduction in *Caenorhabditis elegans. Nature* **367,** 467–470 (1994).
14. Waldmann, R., Champigny, G., Voilley, N., Lauritzen, I. & Lazdunski, M. The mammalian degenerin MDEG, an amiloride-sensitive cation channel activated by mutations causing neurodegeneration in *Caenorhabditis elegans. J. Biol. Chem.* **271,** 10433–10434 (1996).
15. Kovalchuk Yu, N., Krishtal, O. A. & Nowycky, M. C. The proton-activated inward current of rat sensory neurons includes a calcium component. *Neurosci. Lett.* **115,** 237–242 (1990).
16. Konnerth, A., Lux, H. D. & Morad, M. Proton-induced transformation of calcium channel in chick dorsal root ganglion cells. *J. Physiol.* **386,** 603–633 (1987).
17. Davies, N. W., Lux, H. D. & Morad, M. Site and mechanism of activation of proton-induced sodium current in chick dorsal root ganglion neurones. *J. Physiol.* **400,** 159–187 (1988).
18. Korkushko, A. & Kryshtal, O. Blocking of proton-activated sodium permeability of the membranes of trigeminal ganglion neurons in the rat by organic cations. *Neirofiziologiia* **16,** 557–561 (1984).
19. Grantyn, R., Perouansky, M., Rodriguez-Tebar, A. & Lux, H. D. Expression of depolarizing voltage- and transmitter-activated currents in neuronal precursor cells from the rat brain is preceded by a proton-activated sodium current. *Dev. Brain Res.* **49,** 150–155 (1989).
20. Price, M. P., Snyder, P. M. & Welsh, M. J. Cloning and expression of a novel human brain Na^+ channel. *J. Biol. Chem.* **271,** 7879–7882 (1996).
21. Akaike, N. & Ueno, S. Proton-induced current in neuronal cells. *Prog. Neurobiol.* **43,** 73–83 (1994).
22. Krishtal, O. A., Osipchuk, Y. V., Shelest, T. N. & Smirnoff, S. V. Rapid extracellular pH transients related to synaptic transmission in rat hippocampal slices. *Brain Res.* **436,** 352–356 (1987).
23. Chesler, M. & Kaila, K. Modulation of pH by neuronal activity. *Trends Neurosci.* **15,** 396–402 (1992).
24. Bevan, S. & Yeats, J. Protons activate a cation conductance in a sub-population of rat dorsal root ganglion neurones. *J. Physiol.* **433,** 145–161 (1991).
25. Lewis, C. *et al.* Coexpression of P2X2 and P2X3 receptor subunits can account for ATP-gated currents in sensory neurons. *Nature* **377,** 432–435 (1995).
26. Barnard, E. A. The transmitter-gated channels: a range of receptor types and structures. *Trends Pharmacol. Sci.* **17,** 305–309 (1996).
27. Okada, Y., Miyamoto, T. & Sato, T. Activation of a cation conductance by acetic acid in taste cells isolated from the bullfrog. *J. Exp. Biol.* **187,** 19–32 (1994).
28. Liu, J., Schrank, B. & Waterson, R. Interaction between a putative mechanosensory membrane channel and a collagen. *Science* **273,** 361–364 (1996).
29. Waldmann, R., Champigny, G. & Lazdunski, M. Functional degenerin-containing chimeras identify residues essential for amiloride-sensitive Na^+ channel function. *J. Biol. Chem.* **270,** 11735–11737 (1995).
30. Renard, S., Lingueglia, E., Voilley, N., Lazdunski, M. & Barbry, P. Biochemical analysis of the membrane topology of the amiloride-sensitive Na^+ channel. *J. Biol. Chem.* **269,** 12981–12986 (1994).

Acknowledgements. This work was supported by the Centre National de la Recherche Scientifique (CNRS) and the Association Française contre les Myopathies (AFM). We thank J. R. de Weille and E. Lingueglia for discussion, G. Jarretou, M. Jodar and N. Leroudier for technical assistance, Y. Benhamou for secretarial assistance, and F. Aguila for help with artwork.

Correspondence and requests for materials should be addressed to M.L. (e-mail: ipmc@unice.fr).

Ras signalling linked to the cell-cycle machinery by the retinoblastoma protein

Daniel S. Peeper*†, Todd M. Upton*, Mohamed H. Ladha*, Elizabeth Neuman*, Juan Zalvide*, René Bernards†, James A. DeCaprio* & Mark E. Ewen*

** The Dana-Farber Cancer Institute and the Harvard Medical School, 44 Binney Street, Boston, Massachusetts 02115, USA*
† The Netherlands Cancer Institute, Department of Molecular Carcinogenesis, Plesmanlaan 121, 1066 CX Amsterdam, The Netherlands

The Ras proto-oncogene is a central component of mitogenic signal-transduction pathways, and is essential for cells both to leave a quiescent state (G0) and to pass through the G1/S transition of the cell cycle[1–6]. The mechanism by which Ras signalling regulates cell-cycle progression is unclear, however. Here we report that the retinoblastoma tumour-suppressor protein (Rb), a regulator of G1 exit[7], functionally links Ras to passage through the G1 phase. Inactivation of Ras in cycling cells caused a decline in cyclin D1 protein levels, accumulation of the hypophosphorylated, growth-suppressive form of Rb, and G1 arrest. When Rb was disrupted either genetically or biochemically, cells failed to arrest in G1 following Ras inactivation. In contrast, inactivation of Ras in quiescent cells prevented growth-factor induction of both immediate-early gene transcription and exit from G0 in an Rb-independent manner. These data suggest that Rb is an essential G1-specific mediator that links Ras-dependent mitogenic signalling to cell-cycle regulation.

The function of Ras was neutralized to examine whether the resulting inhibition of proliferation requires Rb function. By inhibiting rather than activating Ras signalling, we could identify target proteins that are critical for, rather than proteins whose function correlates with, Ras-dependent effects on the cell cycle. Asynchronous primary $Rb^{+/+}$ and $Rb^{-/-}$ mouse embryo fibroblasts (MEFs) were microinjected with monoclonal antibody Y13-259, which specifically neutralizes Ras[4,8], and DNA replication was monitored by incorporation of 5-bromodeoxyuridine (BrdU). Neutralization of Ras led to efficient inhibition of DNA synthesis in the $Rb^{+/+}$ MEFs (Fig. 1a). In contrast, inactivation of Ras led to a sevenfold smaller inhibition of DNA synthesis in $Rb^{-/-}$ MEFs, a difference similar to that previously reported for microinjection of plasmids encoding p16, an inhibitor of Cdk4 and Cdk6, into both cell types[9,10]. Ras antibody also inhibited the proliferation of immortalized 3T3 derivatives of the $Rb^{+/+}$ and $Rb^{-/-}$ MEFs in an Rb-dependent manner (Fig. 1b). Similar results were obtained for injections of G1 cells after release from a serum-starved state (not shown). These results suggest that the status of Rb can dictate whether cells stop cell-cycle progression in response to inactivation of Ras.

As an independent measure to evaluate the role of Rb in Ras-dependent cell-cycle progression, we co-transfected an expression vector for a dominant interfering Ras mutant, Ras^{Asn17} (refs 11, 12), with a CD20 cell-surface marker and analysed the cell-cycle profile of the transfected population by two-colour flow cytometry. Expression of Ras^{Asn17} caused a significant arrest in the G1 phase of the cell-cycle in NIH 3T3 cells (Fig. 2a). In contrast, expression of Ras^{Asn17} failed to cause G1 arrest in three independent $Rb^{-/-}$ 3T3 clones (Fig. 2a, b), although it was expressed to comparable levels in NIH 3T3 and $Rb^{-/-}$ cells (Fig. 2a). Even higher levels of Ras^{Asn17} (obtained using stronger promoters) failed to stop $Rb^{-/-}$ 3T3 cells from proliferating (data not shown). In agreement with these results, expression of Ras^{Asn17} also led to Rb-dependent inhibition of proliferation in long-term growth-suppression assays (data not shown).

To extend these observations to another cell type, we compared the effect of Ras inactivation in the $Rb^{-/-}$ myoblast cell line CC42 with that in the Rb-positive myoblast cell line C2C12. Expression of Ras^{Asn17} caused significant G1 arrest in C2C12 cells, but not in CC42 cells (Fig. 2c). Similarly, microinjection of neutralizing Ras antibodies resulted in an approximately ninefold greater inhibition of DNA synthesis in C2C12 cells than in CC42 cells (data not shown), providing further support for the results described above.

We then attempted to exclude the possibility that $Rb^{-/-}$ cells might fail to respond to proliferation-restraining signals in general. Consistent with previous reports[9,10,13,14], p16 caused G1 arrest in an Rb-dependent manner (Fig. 2a). In contrast, both a dominant-negative Cdk3 mutant (Cdk3-dn) and the Cdk inhibitor p27, both of which cause cell-cycle arrest in an Rb-independent manner[15], induced G1 arrest as efficiently in $Rb^{-/-}$ 3T3 cells as in NIH 3T3 cells (Fig. 2a). These data indicate that the Rb requirement for induction of G1 arrest is specific for Ras^{Asn17} and p16.

To further exclude the possibility that an Rb-independent mechanism might be responsible for the failure of $Rb^{-/-}$ cells to stop proliferating in response to Ras inactivation, we performed two types of experiments. First, when Rb function was restored in $Rb^{-/-}$

cells, the ability of Ras^{Asn17} to induce G1 arrest as a function of exogenous Rb expression, and vice versa, was monitored. Ras^{Asn17} and Rb, when expressed alone, caused only a small increase in the proportion of G1 cells (Fig. 3). In contrast, in both experimental settings, coexpression of Ras^{Asn17} and Rb induced G1 arrest in a cooperative, rather than additive, fashion. Second, reversal of a Ras^{Asn17}-induced G1 arrest by the adenovirus E1A protein was largely dependent on its Rb-family binding domains (data not shown). Thus either transient inactivation or restoration of Rb can determine the response to downregulated Ras activity. It is therefore unlikely that $Rb^{-/-}$ fibroblasts have acquired an adaptive mutation that renders them unresponsive to Ras signalling.

The above results suggest that, in a cycling asynchronous population of cells, inactivation of Ras causes G1 arrest in an Rb-dependent manner. Previous work suggests that Ras activity is required for immediate-early gene activation and exit from a quiescent (G0) state[4,8,12]. We therefore examined whether Rb is involved in either of these two processes. Ras^{Asn17} completely blocked growth-factor induction of immediate-early gene transcription in $Rb^{-/-}$ 3T3 cells (Fig. 4a), as in NIH 3T3 cells[12]. Moreover, inactivation of Ras prevented growth factor-stimulated cell-cycle re-entry of quiescent $Rb^{-/-}$ 3T3 cells (Fig. 4b, c). These results are consistent with the observation that primary $Rb^{-/-}$ MEFs and $Rb^{-/-}$ 3T3 cells can be arrested by serum deprivation[16,17] (Fig. 4). Furthermore, these data indicate that, in $Rb^{-/-}$ 3T3 cells, Ras signalling can be blocked by either Ras^{Asn17} or Ras antibody. More importantly they suggest that Rb is a critical component of Ras-dependent signalling during G1 but not G0.

Our results suggest that inactivation of Ras prevents G1 exit by

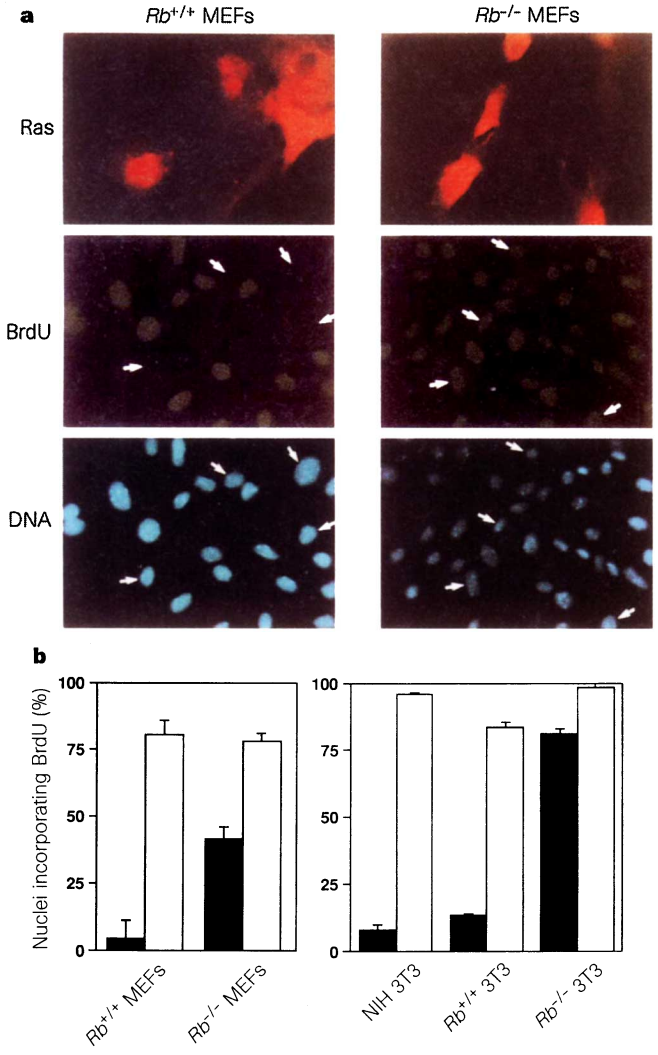

Figure 1 Microinjection of Ras-neutralizing antibody inhibits cell-cycle progression in an Rb-dependent manner. **a**, Ras-neutralizing antibody inhibits DNA synthesis in $Rb^{+/+}$ MEFs but not $Rb^{-/-}$ MEFs. Ras monoclonal antibody (Y13-259) was microinjected into the cytoplasm of asynchronous cultures of primary MEFs derived from $Rb^{+/+}$ (left) or $Rb^{-/-}$ (right) mouse embryo littermates (nuclei of injected cells are indicated by arrows). Top, staining for immunoglobulin-positive, injected cells. Middle, identical field stained for 5-bromodeoxyuridine (BrdU). Bottom, nuclear counterstaining with DAPI. **b**, Percentage of BrdU-incorporating cells after microinjection with Ras antibody (filled bars) or control IgG (open bars). As well as primary MEFs (left), immortalized (3T3) fibroblasts derived from $Rb^{+/+}$ and $Rb^{-/-}$ mouse embryos, and NIH 3T3 cells were used (right). At least 400 microinjected cells were assayed per cell type and antibody used. The results show mean + s.e. for at least four independent experiments.

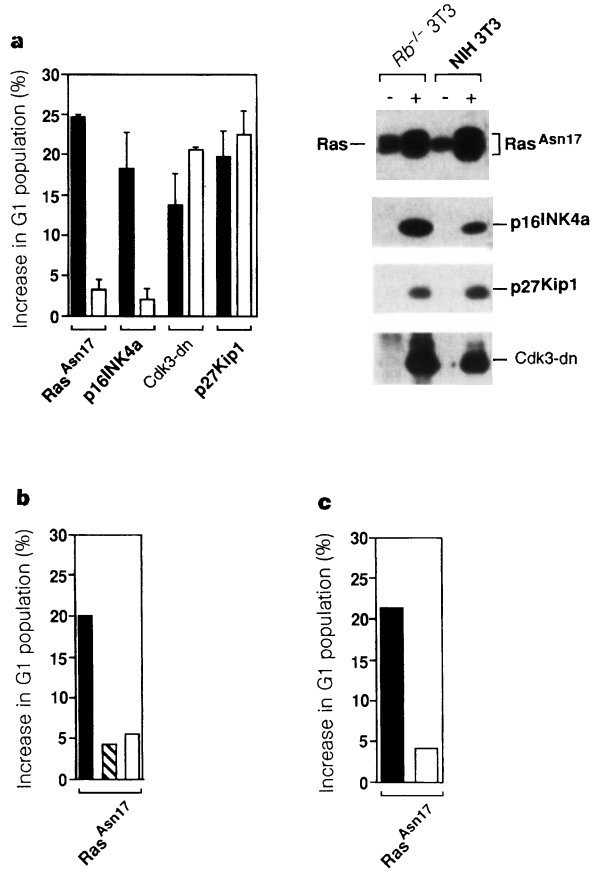

Figure 2 Expression of Ras^{Asn17} causes G1 cell-cycle arrest in an Rb-dependent manner. **a**, Left, NIH 3T3 cells (filled bars) and $Rb^{-/-}$ 3T3 cells (open bars) were transfected with control plasmid, or with plasmids as indicated, together with a plasmid encoding the CD20 cell-surface marker. The transfected cell population was identified by staining with fluorescein isothiocyanate (FITC)-conjugated anti-CD20 antibody and DNA content was monitored by staining with propidium iodide and two-colour flow cytometry. The absolute changes in the percentage of cells in G1 compared to control transfections are shown with the mean + s.e. from at least three independent experiments. Right, ectopic expression of Ras^{Asn17}, p16, p27 and Cdk3-dn-HA in NIH 3T3 and $Rb^{-/-}$ 3T3 cells, as visualized by immunoprecipitation, SDS–PAGE and autoradiography; − and + indicate control (vector) and expression plasmid transfections, respectively. **b**, As **a**, performed with two other independently derived immortalized $Rb^{-/-}$ 3T3 cell populations (hatched and open bars), relative to NIH 3T3 cells (filled bar). A representative experiment is shown. **c**, As **a**, performed with the Rb-positive myoblast cell line C2C12 (filled bars) and the $Rb^{-/-}$ myoblast cell line CC42 (open bars).

modulating Rb activity. To test this, we determined whether expression of Ras^{Asn17} affects the phosphorylation status of Rb. When expressed ectopically in NIH 3T3 cells, Rb migrated as a doublet, suggesting that both hypophosphorylated (growth-suppressive) and hyperphosphorylated (inactive) Rb species were present in roughly equimolar amounts (Fig. 5a). In contrast, when coexpressed with Ras^{Asn17}, Rb accumulated almost exclusively in its hypophosphorylated form, suggesting that inhibition of Ras activity leads to inhibition of Rb phosphorylation.

The accumulation of cyclin D proteins, the regulatory subunits of Cdk4 and Cdk6 that phosphorylate Rb, is regulated in part by mitogens[18]. This finding, together with the above results, prompted us to examine whether Ras inactivation decreases the accumulation of cyclin D1 protein. Indeed, a significant reduction in cyclin D1 protein levels was observed when Ras^{Asn17} was expressed (Fig. 5b, left). This effect was specific for cyclin D1, as Ras inactivation did not affect the expression of either Cdk4 or tubulin. Moreover, a Cdk2-dn-induced G1 arrest did not result in a reduction of cyclin D1. Importantly, expression of Ras^{Asn17} in $Rb^{-/-}$ 3T3 cells also led to a decline in cyclin D1 (Fig. 5b, right). Because proliferating $Rb^{-/-}$ 3T3 cells do not undergo G1 arrest when Ras is inactivated (Figs 1, 2 and 3), this result uncouples downregulation of cyclin D1 by Ras^{Asn17} from any cell-cycle effects, and indicates that the signalling pathway between Ras and cyclin D1 in $Rb^{-/-}$ 3T3 cells is intact.

To examine whether it is the decline in cyclin D1 that causes inhibition of Rb phosphorylation when Ras is inactivated, we monitored the effect of individual G1 kinase subunits on Rb phosphorylation in this setting. Coexpression with either Cdk4 or Cdk2 alone did not have a significant effect on the inhibition of Rb phosphorylation by Ras^{Asn17} (Fig. 5a), consistent with the observation that Cdk4 levels are not altered by Ras^{Asn17} expression (Fig. 5b). In contrast, coexpression of cyclins D1, D2 or E rescued the inhibition of Rb phosphorylation by Ras^{Asn17}. This suggests that Ras inactivation causes downregulation of cyclin D1, which in turn leads to the accumulation of hypophosphorylated and active Rb, preventing G1 exit.

We then prevented the downregulation of cyclin D1 to determine whether it is an essential step during the induction of G1 arrest by Ras inactivation. Both cyclin D1-Cdk4 and cyclin D2-Cdk4, as well as activated Ras^{Val12}, completely overcame Ras^{Asn17}-induced G1 arrest, either in the absence or presence of nocodazole (Fig. 5c, d). This suggests that downregulation of cyclin D1 is required for Ras^{Asn17} to induce cell-cycle arrest. These observations are consistent with previous reports on the regulation of cyclin D1 transcription[19,20], that induction of cyclin D1 by oncogenic Ras may contribute to transformation[21–23], and that p16 blocks Ras plus Myc-induced transformation[24]. Cyclin E-Cdk2 was less effective than cyclin D-Cdk4 in reversing the G1 arrest induced by Ras^{Asn17}. A possible explanation for this is the suggested coordinate action of cyclin D- and E-dependent kinases in the complete phosphorylation and inactivation of Rb[25]. Without initial phosphorylation of Rb by cyclin D kinases, cyclin E-Cdk2 may be capable of only partly phosphorylating (and inactivating) Rb. However, this may be sufficient to cause a shift of Rb on a denaturing gel (Fig. 5a).

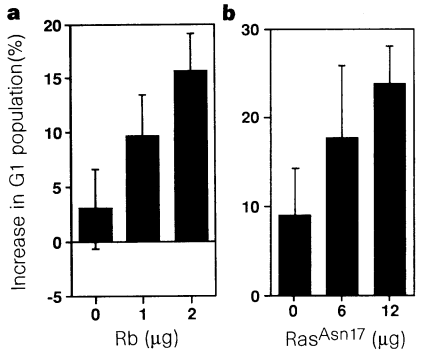

Figure 3 Reintroduction of Rb into $Rb^{-/-}$ fibroblasts rescues induction of G1 arrest by Ras inactivation. **a**, Individual cell populations of $Rb^{-/-}$ 3T3 cells were transfected with a constant amount of plasmids expressing Ras^{Asn17} and CD20, together with an increasing amount of a plasmid encoding Rb. After transfection, cells were processed and the absolute change in the percentage of cells in G1, relative to a control transfection, was determined by FACS analysis. Data were corrected for cell-cycle effects caused by expression of Rb alone; mean + s.e. for four independent experiments. **b**, As **a**, except Rb plasmid was held constant and Ras^{Asn17} expression plasmid was added in increasing amounts. Cell-cycle effects caused by expression of Ras^{Asn17}, in the absence of Rb, were corrected for; mean + s.e. for two independent experiments.

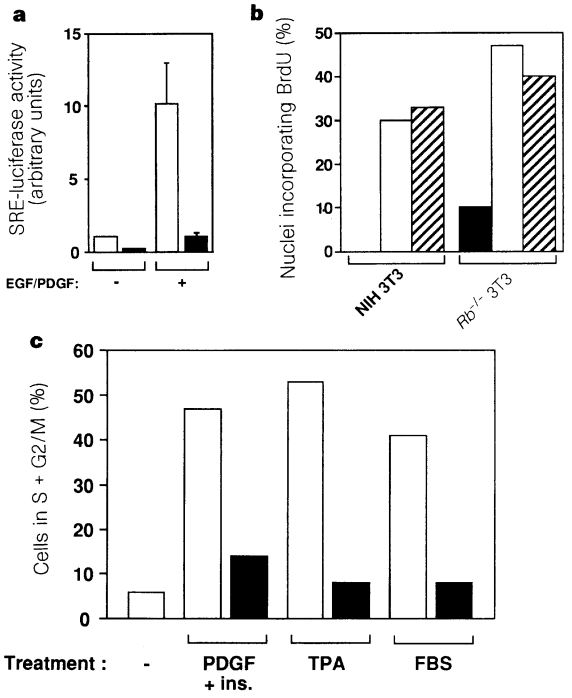

Figure 4 Inhibition of Ras activity blocks G0 exit in an Rb-independent manner. **a**, Ras^{Asn17} expression inhibits growth factor-induced serum response element (SRE) activity in $Rb^{-/-}$ 3T3 cells. $Rb^{-/-}$ 3T3 cells were transfected with Ras^{Asn17} expression plasmid (filled bars) or empty vector (open bars), together with an SRE-luciferase reporter plasmid. Then, 24 h after transfection, cells were serum starved (0.1% FBS) for 72 h. At this time, no growth factors or PDGF and EGF (10 ng ml^{-1} each) were added to the cultures and luciferase activity was measured 24 h later; mean + s.e. for three independent experiments are shown. Similar results were obtained for NIH 3T3 cells (not shown). **b**, Ras neutralization inhibits growth factor-induced G0 exit in $Rb^{-/-}$ 3T3 cells. Cells rendered quiescent by serum starvation were microinjected with either control (rabbit IgG; open bars) or anti-Ras antibody (filled bars), stimulated with EGF and PDGF (10 ng ml^{-1} each) and analysed for incorporation of BrdU. The absolute percentages of cells incorporating BrdU for each cell type under each condition are shown. Percentages are for over 150 injected cells from at least two independent experiments. The absolute percentage of uninjected cells incorporating BrdU after growth factor stimulation is indicated (hatched bars). **c**, Ras^{Asn17} expression inhibits growth factor-induced G0 exit in $Rb^{-/-}$ 3T3 cells. $Rb^{-/-}$ 3T3 cells were serum starved for 24 h, infected with recombinant Ras^{Asn17} adenovirus (open bars) or control adenovirus (filled bars) as indicated, and starved for another 16 h. Cells were treated with either PDGF (10 ng ml^{-1}) + insulin (ins., 10 μg ml^{-1}), TPA (25 nM) or FBS (2%) and cell-cycle profiles were determined by FACS analysis 22 h later. The absolute percentages of cells in S + G2/M phases are shown. The control (left lane) shows the percentage of cells in S + G2/M just before stimulation.

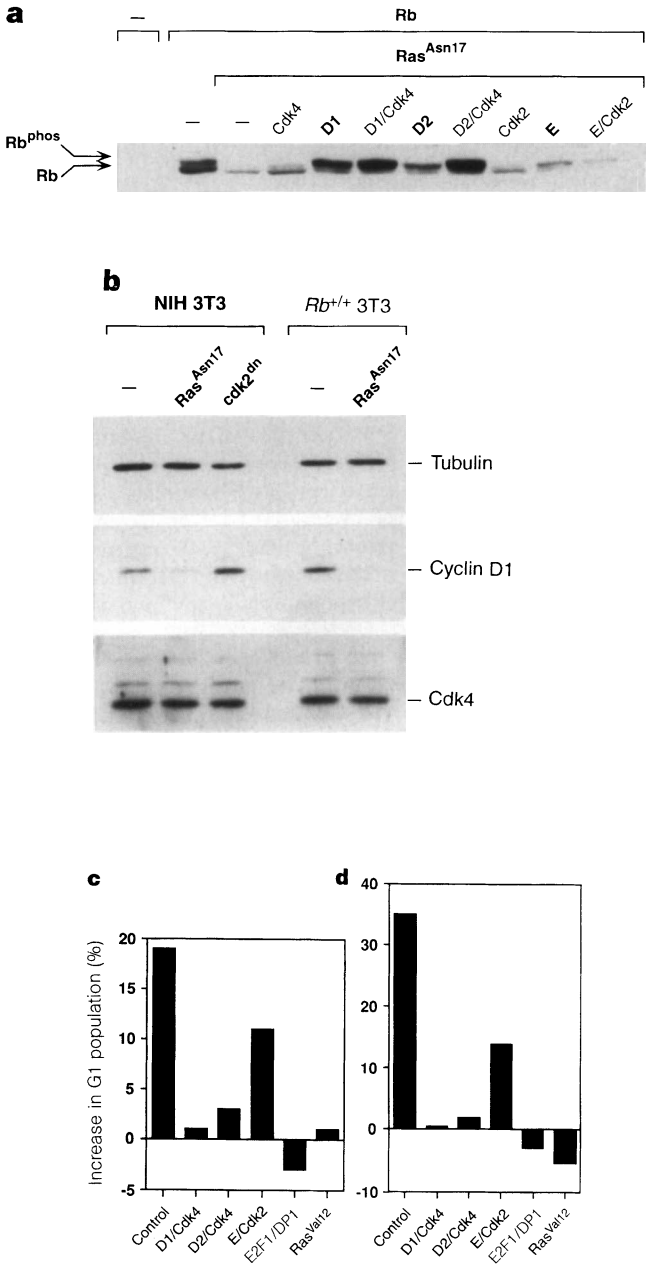

Figure 5 D-type cyclins and E2F overcome the inhibitory effect of Ras inactivation on cell-cycle progression. **a**, NIH 3T3 cells were transfected with plasmid encoding human Rb, either in the absence or presence of expression vectors for Ras^{Asn17} and cyclin-dependent kinase subunits, as indicated. Rb was detected by western blotting. **b**, NIH 3T3 and $Rb^{-/-}$ 3T3 cells were transfected with plasmids encoding either Ras^{Asn17}, a dominant-negative Cdk2 mutant or empty vector, as indicated, together with a plasmid encoding the CD20 cell-surface marker. Extracts from transfected cells isolated by CD20-specific cell sorting were subjected to western blotting with specific antibodies, as indicated. **c**, NIH 3T3 cells were co-transfected with plasmids encoding CD20, Ras^{Asn17} and plasmids encoding cyclin-Cdk kinases, E2F1 and DP1, or Ras^{Val12}, as indicated. As a control, CD20 and Ras^{Asn17} plasmids were co-transfected with empty vector (first lane). The cell-cycle profiles of the transfected cell populations were determined by FACS analysis. A representative experiment from at least three independent experiments, with the absolute change in percentage of cells in G1 compared to control transfections, is shown. **d**, As **c**, except that nocodazole (50 ng ml^{-1}) was added to the cultures 24 h after transfection to reduce the background proportion of cells in G1.

Our results predict that downstream components within the Rb pathway should also interfere with the inhibition of proliferation when Ras is inactivated. The E2F1-DP1 transcription factor, an Rb-effector, completely overcame Ras^{Asn17}-induced G1 arrest (Fig. 5c, d), thus providing additional support for a model in which cyclin D, Rb and E2F are components of a critical Ras-effector pathway. However, more complex signalling networks may be involved in Ras-mediated transformation. Nevertheless, our results suggest that Rb, by acting in a pathway with Ras, is important for adequate growth regulation during antimitogenic Ras-dependent signalling. □

Methods

Microinjection. MEFs isolated from $Rb^{+/+}$ and $Rb^{-/-}$ mouse embryo littermates and their immortalized 3T3 derivatives[26] were cultured in DMEM with 10% FBS. NIH 3T3 cells were cultured in DMEM containing 5% bovine calf serum. Cells were plated onto photo-etched coverslips preincubated in PBS–0.1% gelatin. Asynchronous cells were microinjected with either Ras monoclonal antibody Y13-259 (Oncogene Science) or rabbit IgG (Sigma) at 5 mg ml^{-1} in PBS. At least 100 cells were injected in each experiment. BrdU (10 μM) was added 11–13 h post-injection and processed 24–26 h post-injection. To process microinjected cells for immunofluorescence, coverslips were rinsed twice with PBS and fixed for 10 min with 3% paraformaldehyde in PBS–2% sucrose. Coverlips were then rinsed three times in PBS and cells were permeabiized in PBS–0.2% Triton X-100. Coverslips were then rinsed three times in PBS and blocked for 15–20 min with PBS containing 0.1% Triton X-100 and 3% BSA. This and subsequent washes were done three times in PBS–0.1% Triton X-100. Coverslips were then incubated with either rhodamine-conjugated goat anti-rabbit or rhodamine-conjugated goat anti-rat secondary antibody, diluted 1:200 in blocking buffer, in a humidified chamber for 15 min. After washing, slips were incubated 10 min in 1.5 M HCl. Coverslips were washed and incubated for 30 min in a humidified chamber with anti-BrdU antibody, diluted 1:2.5 in PBS–0.1% Triton X-100. Coverlips were washed and nuclei were stained with DAPI. For analysis of quiescent fibroblasts, cells were maintained in 0.1% FBS for 48 h before microinjection with either control rabbit IgG or anti-Ras antibody. Cells were stimulated with EGF and PDGF 2–4 h post-injection and BrdU was added 8–10 h later. Cells were processed for immunofluorescence 24 h post-injection.

Cell-cycle analysis. To determine cell-cycle effects by Ras^{Asn17} expression, 4 μg pCMV-CD20 was co-transfected with 21 μg of either pMT-Ras^{Asn17} (gift from G. Cooper) or control plasmid pMT-ΔBam into cycling $Rb^{-/-}$ 3T3, NIH 3T3, CC42 (ref. 27; gift from J. Schneider) and C2C12 cells. As controls, 21 μg of either pcDNA3-p16, pCMV-Cdk3-dn-HA (gift from E. Harlow), or pCMV5-p27 (gift from J. Massagué) was co-transfected into $Rb^{-/-}$ 3T3 and NIH 3T3 cells. For fluorescence-activated cell sorting (FACS) analysis, CD20-co-transfected cells were identified with CD20-specific FITC-conjugated antibodies 44 h post-transfection[28]. After propidium iodide staining of DNA, the cell-cycle profiles (2,000–10,000 $CD20^+$ cells per sample) were analysed by FACS on a Becton-Dickinson FACScan machine. For cell-cycle analysis of quiescent $Rb^{-/-}$ 3T3 cells upon growth-factor stimulation, cells were starved in 0.1% FBS for 24 h, infected with recombinant adenoviruses, starved for another 16 h, stimulated for 22 h, and processed. To generate a control plasmid for Ras^{Asn17}, pMT-ΔBam, the entire Ras^{Asn17} coding sequence was removed from pMT-Ras^{Asn17} and the vector was religated. pcDNA3-p16 was generated by inserting an *Eco*RI–*Xho* fragment from pBS-p16 (ref. 29; gift from D. Beach) into pcDNA3 (Invitrogen). In the Rb restoration experiments, $Rb^{-/-}$ 3T3 cells were transfected with 4 μg pCMV-CD20, 12 μg of either pMT-Ras^{Asn17} or pMT-ΔBam, and pCMV-Rb (0, 1 or 2 μg). Alternatively, pCMV-Rb (4 μg) was cotransfected with increasing amounts of pMT-Ras^{Asn17} (0, 6 or 12 μg). To rescue Ras^{Asn17}-induced G1 arrest, 2 μg pCMV-CD20 was co-transfected with 9 μg of either pMT-Ras^{Asn17} or pMT-ΔBam. The following plasmids were co-transfected: 10 μg of cyclin plasmid with 4 μg of Cdk plasmid, 10 μg pCMV-E2F1 with 4 μg pCMV-DP1, 14 μg of pDCR-$Hras^{Val12}$, or pcDNA3. To generate recombinant Ras^{Asn17} adenovirus, Ras^{Asn17} coding sequence was cloned into pCA13 and co-transfected with pBHG10, containing part of the adenoviral genome, into helper cells (Microbix Biosystems, Toronto, Canada).

Immunoprecipitation and western blotting. Immunoprecipitation[28] was

performed with either monoclonal Ras antibody Y13-259, HA monoclonal antibody 12CA5 for Cdk3-dn, p16 monoclonal antibody ZJ11 (Upstate Biotechnology) or p27 polyclonal antibody (M-197, Santa Cruz). To determine Rb phosphorylation status, 8 μg of pCMV-Rb was co-transfected with 8 μg of either pMT-Ras^{Asn17} or pMT-ΔBam. Plasmids (6 μg) for cyclins D1, D2 (ref. 28) or E (gift from R. Weinberg) subcloned into pRc/CMV (Invitrogen), or 3 μg for Cdk (pCMV-Cdk4-HA or pCMV-Cdk2 (gift from E. Harlow)) plasmid were co-transfected. To determine the effect of Ras^{Asn17} on specific cellular proteins, 5 μg of pCMV-CD20 was co-transfected with 5 μg pcDNA3 and 15 μg of pMT-Ras^{Asn17}, pMT-ΔBam or pCMV-Cdk2-dn (gift from E. Harlow). For cell sorting, cells were processed 44 h after transfection, and the CD20-positive population was isolated on a Becton-Dickinson Cell Sort machine, lysed and used for western blotting (80,000 cells) with antibodies; Rb (C15, Santa Cruz), cyclin D1 (DSC-6, Sanbyo), rabbit antiserum for Cdk4 (gift from C. Sherr), or anti-tubulin antibody YL1/2 (ECACC).

Luciferase assays. Cells were co-transfected with 5 μg pSRE-luc (gift from R. Davis) and either 15 μg pMT-Ras^{Asn17} or pMT-ΔBam, and 5 μg CMV-βgal. Cells were incubated 20 h post-transfection in DMEM containing 0.1% FBS. After 3 days, cells were stimulated with EGF and PDGF (R&D Systems), and luciferase activity was measured 24 h later[30].

Received 29 August 1996; accepted 10 January 1997.

1. Pardee, A. B. G1 events and regulation of cell proliferation. *Science* **246,** 603–608 (1989).
2. Pronk, G. J. & Bos, J. L. The role of p21ras in receptor tyrosine kinase signalling. *Biochim. Biophys. Acta* **1198,** 131–147 (1994).
3. Marshall, C. J. Specificity of receptor tyrosine kinase signalling: transient versus sustained extracellular signal-regulated kinase activation. *Cell* **80,** 179–185 (1995).
4. Dobrowolski, S., Harter, M. & Stacey, D. W. Cellular ras activity is required for passage through multiple points of the G0/G1 phase in Balb/c 3T3 cells. *Mol. Cell. Biol.* **14,** 5441–5449 (1994).
5. Feramisco, J. R., Gross, M., Kamata, T., Rosenberg, M. & Sweet, R. W. Microinjection of the oncogene form of the human H-ras (T-24) protein results in rapid proliferation of quiescent cells. *Cell* **38,** 109–117 (1984).
6. Stacey, D. W. & Kung, H. F. Transformation of NIH 3T3 cells by microinjection of Ha-ras protein. *Nature* **310,** 508–511 (1984).
7. Weinberg, R. A. The retinoblastoma protein and cell cycle control. *Cell* **81,** 323–330 (1995).
8. Mulcahy, L. S., Smith, M. R. & Stacey, D. W. Requirement for ras proto-oncogene function during serum-stimulated growth of NIH 3T3 cells. *Nature* **313,** 241–243 (1985).
9. Lukas, J. *et al.* Retinoblastoma-protein-dependent cell-cycle inhibition by the tumour suppressor p16. *Nature* **375,** 503–506 (1995).
10. Koh, J., Enders, G. H., Dynlacht, B. D. & Harlow, E. Tumour-derived p16 alleles encoding proteins defective in cell-cycle inhibition. *Nature* **375,** 506–510 (1995).
11. Feig, L. A. & Cooper, G. M. Inhibition of NIH 3T3 cell proliferation by a mutant ras protein with preferential affinity for GDP. *Mol. Cell. Biol.* **8,** 3235–3243 (1988).
12. Cai, H., Szeberenyi, J. & Cooper, G. M. Effect of a dominant inhibitory Ha-ras mutation on mitogenic signal transduction. *Mol. Cell. Biol.* **10,** 5314–5323 (1990).
13. Medema, R. H., Herrera, R. E., Lam, F. & Weinberg, R. A. Growth suppression by p16ink4 requires functional retinoblastoma protein. *Proc. Natl Acad. Sci. USA* **92,** 6289–6293 (1995).
14. Guan, K.-L. *et al.* Growth suppression by p18, a p16INK4/MTS1- and p14INK4B/MTS2-related CDK6 inhibitor, correlates with wild-type pRb function. *Genes Dev.* **8,** 2939–2952 (1994).
15. Sherr, C. J. & Roberts, J. M. Inhibitors of mammalian G1 cyclin-dependent kinases. *Genes Dev.* **9,** 1149–1163 (1995).
16. Herrera, R. E. *et al.* Altered cell cycle kinetics, gene expression, and G1 restriction point regulation in Rb-deficient fibroblasts. *Mol. Cell. Biol.* **16,** 2402–2407 (1996).
17. Lukas, J., Bartkova, J., Rohde, M., Strauss, M. & Bartek, J. Cyclin D1 is dispensable for G1 control in retinoblastoma gene-deficient cells independently of cdk4 activity. *Mol. Cell. Biol.* **15,** 2600–2611 (1995).
18. Sherr, C. J. Mammalian G1 cyclins. *Cell* **73,** 1059–1065 (1993).
19. Lavoie, J. N., L'Allemain, G., Brunet, A., Muller, R. & Pouysségur, J. Cyclin D1 expression is regulated positively by the p42/p44MAPK and negatively by the p38/HOGMAPK pathway. *J. Biol. Chem.* **271,** 20608–20616 (1966).
20. Albanese, C. *et al.* Transforming p21ras mutants and c-Ets-2 activate the cyclin D1 promoter through distinguishable regions. *J. Biol. Chem.* **270,** 23589–23597 (1995).
21. Filmus, J. *et al.* Induction of cyclin D1 overexpression by activated ras. *Oncogene* **9,** 3627–3633 (1994).
22. Liu, J.-J. *et al.* Ras transformation results in an elevated level of cyclin D1 and acceleration of G1 progression in NIH 3T3 cells. *Mol. Cell. Biol.* **15,** 3654–3663 (1995).
23. Winston, J. T., Coats, S. R., Wang, Y.-Z. & Pledger, W. J. Regulation of the cell cycle machinery by oncogenic Ras. *Oncogene* **12,** 127–134 (1996).
24. Serrano, M., Gomez-Lohoz, E., DePinho, R. A., Beach, D. & Bar-Sagi, D. Inhibition of Ras-induced proliferation and transformation by p16INK4. *Science* **267,** 249–252 (1995).
25. Hatakeyama, M., Brill, J. A., Fink, G. R. & Weinberg, R. A. Collaboration of G1 cyclins in the functional inactivation of the retinoblastoma protein. *Genes Dev.* **8,** 1759–1771 (1994).
26. Zalvide, J. & DeCaprio, J. A. Role of pRb-related proteins in simian virus 40 large-T-antigen-mediated transformation. *Mol. Cell. Biol.* **15,** 5800–5810 (1995).
27. Schneider, J. W., Gu, W., Zhu, L., Mahdavi, V. & Nadal-Ginard, B. Reversal of terminal differentiation mediated by p107 in Rb$^{-/-}$ muscle cells. *Science* **264,** 1467–1471 (1994).
28. Ewen, M. E. *et al.* Functional interactions of the retinoblastoma protein with mammalian D-type cyclins. *Cell* **73,** 487–497 (1993).
29. Serrano, M., Hannon, G. J. & Beach, D. A new regulatory motif in cell-cycle control causing specific inhibition of cyclin D/cdk4. *Nature* **366,** 704–707 (1993).
30. Ewen, M. E., Oliver, C. J., Sluss, H. K., Miller, S. J. & Peeper, D. S. p53-dependent repression of CDK4 translation in TGF-β-induced cell-cycle arrest. *Genes Dev.* **9,** 204–217 (1995).

Acknowledgements. D.S.P. and T.M.U. contributed equally to this work. We thank R. Medema for critical ideas; D. Livingston, P. Adams, D. Ginsberg, R. Scully, S. Bhattacharya, W. Sellers and our colleagues in the Ewen and Bernards laboratories for criticism and encouragement; P. Adams, D. Beach, G. Cooper, R. Davis, T. Ernst, E. Harlow, P. Hinds, P. Hordijk, T. Jacks, W. Kaelin, O. Kranenburg, W. Krek, J. Massagué, H. Masselink, J. Schneider, C. Sherr, M. Voorhoeve, R. Weinberg, E. White, Y. Xiong and R. Zwijsen for plasmids, antibodies, cell lines, growth factors, mice and help wtih generating recombinant adenovirus; and members of the flow-cytometry facilities for their help. D.S.P. thanks Y. C. Peeper for support. D.S.P. is a fellow of the Dutch Cancer Society. E.N. is supported by a fellowship from the Woman's Cancers Program at the Dana-Farber Cancer Institute. This work was supported by grants from the NIH and the Sandoz/Dana-Farber Drug Discovery Program (M.E.E.).

Correspondence and requests for materials should be addressed to M.E.E. (e-mail: mark_ewen@dfci.harvard.edu).

A family of proteins that inhibit signalling through tyrosine kinase receptors

Alexei Kharitonenkov*†, Zhengjun Chen*†, Irmi Sures†, Hongyang Wang†, James Schilling‡ & Axel Ullrich†

† *Department of Molecular Biology, Max-Planck-Institute für Biochemie, Am Klopferspitz 18A, 82152 Martinsried, Germany*
‡ *Sugen Inc., 515 Galveston Road, Redwood City, California 94063, USA*
* *These authors contributed equally to this work*

Phosphotyrosine phosphatases are critical negative or positive regulators in the intracellular signalling pathways that result in growth-factor-specific cell responses such as mitosis, differentiation, migration, survival, transformation or death[1–4]. The SH2-domain-containing phosphotyrosine phosphatase SHP-2 is a positive signal transducer for several receptor tyrosine kinases (RTKs) and cytokine receptors[5–7]. To investigate its mechanism of action we purified a tyrosine-phosphorylated glycoprotein which in different cell types associates tightly with SHP-2 and appears to serve as its substrate. Peptide sequencing in conjunction with complementary DNA cloning revealed a new gene family of at least fifteen members designated signal-regulatory proteins (SIRPs). They consist of two subtypes distinguished by the presence or absence of a cytoplasmic SHP-2-binding domain. The transmembrane polypeptide SIRPα1 is a substrate of activated RTKs and in its tyrosine-phosphorylated form binds SHP-2 through SH2 interactions and acts as its substrate. It also binds SHP-1 and Grb2 *in vitro* and has negative regulatory effects on cellular responses induced by growth factors, oncogenes or insulin. Our findings indicate that proteins belonging to the SIRP family generally regulate signals defining different physiological and pathological processes.

Analysis of anti-SHP-2 immunoprecipitates from both pervanadate (POV) as well as growth-factor-stimulated cells revealed a major tyrosine-phosphorylated protein. In mouse mammary tumour (MM5/C1) cells, Rat1 cells overexpressing the human insulin receptor (Rat1-IR) and human epidermoid carcinoma (A431) cells, this phosphoprotein migrated at positions corresponding to relative molecular masses of 120K, 110K and 90K, respectively (Fig. 1a), which upon *in vitro* deglycosylation was in all cases reduced to 65K. This indicated that the same 65K SHP-2-binding protein was differentially glycosylated in a species-specific manner. In some cell lines, for example in A431 cells, other tyrosine-phosphorylated proteins in the 90K–120K range were unaffected by the deglycosylation treatment (Fig. 1b) and may in fact be Gab1 (ref. 8) and/or the human homologue of the *Drosophila* DOS protein[9]. Insulin-treated Rat1-IR cells were used to purify the 110K SHP-2-binding glycoprotein (Fig. 1b, right) by standard chromatography procedures (see Methods). About 4 μg of the semi-pure glycoprotein that copurified with SHP-2 (Fig. 1c) was subjected to microsequence analysis: this yielded five peptide sequences. Computer-aided search for the corresponding DNAs in the expressed-sequence tag (EST) database led to the identification of a 305-base-pair (bp) rat sequence (accession number H31804) and of a human cDNA fragment of 2 kilobases (kb) (EMBL database,